The International Journal of Advanced Manufacturing Technology (2024) 132:63–82
https://doi.org/10.1007/s00170-024-13452-8

CRITICAL REVIEW

Corrosion characteristics of high-entropy alloys prepared by spark plasma sintering

Chika Oliver Ujah[1,2] · **Daramy V. V. Kallon**[1] · **Victor Sunday Aigbodion**[2,3,4]

Received: 16 January 2024 / Accepted: 13 March 2024 / Published online: 19 March 2024

Abstract
High-entropy alloys (HEAs) are special type of alloy suitably developed for use in petroleum exploration, energy storage devices, medical implants, etc. This is because they possess excellent corrosion, thermal, and mechanical properties. Corrosion characteristic of HEAs prepared via spark plasma sintering is a top notch as the technique generates corrosion resistant phases and homogenous microstructure. This study was aimed at reviewing recent publications on corrosion characteristics of HEAs processed by SPS in order to develop ways of improving their anti-corrosion properties. The resource materials were obtained from Scopus-indexed journals and Google Scholar websites of peer-reviewed articles published within the last 5 years. From the study, it was revealed that incorporation of some elements (Al, Cr, Ti) into HEAs can improve their corrosion resistance, while addition of some others can reduce their brittleness and enhance their stability and formability. It was recommended that optimization of SPS parameters was one of the strategies of generating better corrosion characteristics in HEAs.

Keywords Corrosion · High-entropy alloys · Intermetallics · Passive film · Spark plasma sintering

1 Introduction

The development of stainless steel came to be because mild steel is susceptible to corrosion. Likewise, titanium alloy was developed because pristine Ti cannot withstand high-temperature oxidation. Reinforcement of monolithic elements is always undertaken to improve some properties in the substrate (matrix) or introduce a new property. It is from this background that high-entropy alloy was conceived and invented. High-entropy alloys (HEAs) are typical metallic alloys comprising of 5 elements or more combined in equiatomic or near-equiatomic composition (Fig. 1). Each element in the alloy possesses an atomic concentration of 5–35%. The entropy of formation is very high, and this attribute contributes to their exceptional characteristics. Their enthalpy of formation is generally small in comparison with that of conventional alloys, and this contributes to their metastable structural configuration. Hitherto, scholars were saddled with the traditional alloys' challenges, such as high-temperature oxidation, high-temperature creep, and loss of strength at high temperatures which undermined their applications in aerospace, automotive, electrical, and structural systems. So, the burning zeal to develop a more robust material via research and innovation led to the discovery of this all-important alloy. Recall that conventional alloys like Ni, Ti, and Al alloys exhibited depreciation of strength when used at temperatures between 350 and 650 °C. That made their performance at these temperatures poor, and this contributed to their failure in aerospace, automotive, and structural components [1–6]. The first mention of HEAs was in two independently published articles in 2004 by Yeh and Cantor. From then, the study of HEAs had grown geometrically [7, 8].

✉ Chika Oliver Ujah
chikau@uj.ac.za

1 Department of Mechanical and Industrial Engineering Technology, University of Johannesburg, P.O. Box 524, Johannesburg 2006, South Africa

2 Africa Centre of Excellence for Sustainable Power and Energy Development (ACE-SPED), University of Nigeria, Nsukka 410001, Nigeria

3 Faculty of Engineering and Built Environment, University of Johannesburg, P.O. Box 524, Johannesburg 2006, South Africa

4 Department of Metallurgical and Materials Engineering, University of Nigeria, Nsukka 410001, Nigeria

A number of phenomenal effects which occur during the formation of HEAs abound and these contribute to their unique properties. The effects include high entropy, sluggish diffusion, lattice distortion, and cocktail. High entropy effect is the concept which explains that HEAs experience a high degree of randomness during formation which induces unique properties in them than it is experienced in traditional alloys. Such properties include single-phase solid solution, refined microstructure, homogenous and ultra-fine grains. Lattice distortion establishes that the kinetics of HEAs' formation stimulate spinning and straining of atoms domiciled in the lattice configuration and subsequently promote solid solution hardening, grain borderline pinning, and dislocation suppression hardening. The sluggish diffusion effect establishes that HEAs' formation suppresses grain coarsening, reduces phase separation, and enhances thermal strength and creep stability via very slow inter atomic diffusion. Cock tail effect is the concept upholding that each constituent element contributes a particular property to the alloy such that they will synergize to produce some unique properties. It is the combination of all these effects and concepts that bestows unique properties to HEAs [9–13].

Number of publications on HEAs as obtained from Scopus database is shown in Fig. 2. Here, it can be seen that from 2013 to November 2023, 9211 peer-reviewed articles on HEAs (Fig. 2a) and 411 HEAs review articles (Fig. 2b) have been published in journals that are indexed by Scopus. This number excludes conference papers and papers published in other indexing agents. This implies that HEAs have gained a lot of attention, even though more work is still needed to be done because of their importance.

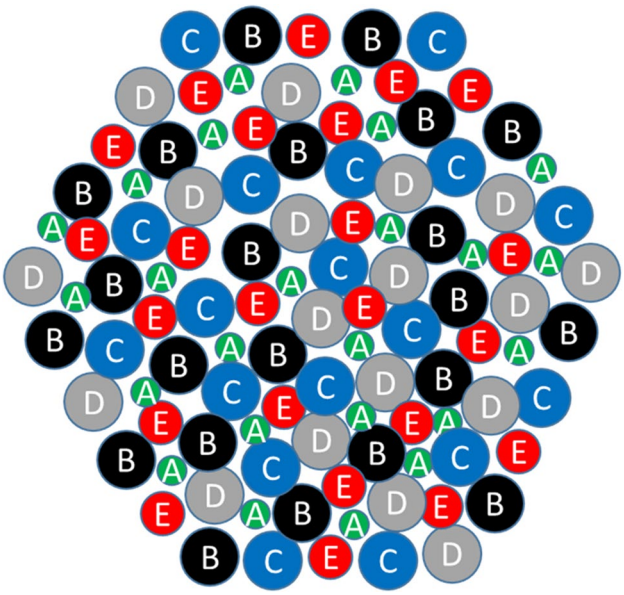

Fig. 1 Schematic diagram of HEA consisting of five elements

Techniques for fabrication of HEAs are manifold and many researchers have reported a number of the processes. Solvo-thermal synthesis was studied by Bondesgaard et al. [14], and other processes include ultrasonic method [15], carbo-thermal shock method [16], and bed pyrolysis [17]. These techniques have not done well in productivity, scalability, energy-saving, and economy. Consequently, diversion of attention to spark plasma sintering (SPS) occurred, and it was reported that it is one of the most robust consolidation processes that is popular in grain refinement, homogenous dispersion of reinforcements, grain boundary interlock, vaporization of impurities, enhancement of microstructure, and good corrosion properties [18–21].

A number of people have worked on SPS of HEAs. Fu et al. [22] produced $Co_{0.5}FeNiCrTi_{0.5}$ alloy by mechanical alloying (MA) and SPS. Results showed enhanced micro hardness with refined microstructure. Yeh et al. [10] noticed that NiCoCrCuFe HEAs prepared via spark plasma sintering generated more improved microstructure and strength than that fabricated with stir casting. Moazzen et al. [23] developed $Fe_XCoCrNi$ ($x = 1–1.6$) alloy using MA and SPS. It was noticed that when Fe fraction was raised, the UTS rose from 480 to 560 mega pascal, while the hardness rose from 320

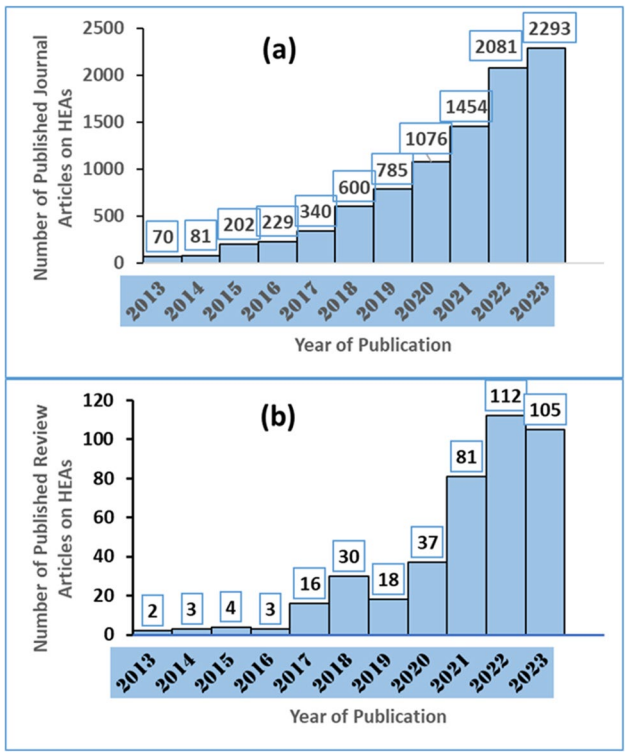

Fig. 2 Publications on HEAs indexed by Scopus from 2013 and 2023: (**a**) publications on HEAs indexed by Scopus excluding conference papers from 2013 to 2023, (**b**) review articles on HEAs from 2013 to November 2023 (data obtained from Scopus database in November 2023 and plotted by the authors)

to 400 Vickers hardness. More so, COF and wear volume diminished tremendously. Exploits of SPS cannot be over emphasized, thus the choice of the technique in this research.

SPS is described as a non-conventional sintering technique employed in powder metallurgy which makes use of pulsed direct current (DC) applied concurrently with axial pressure to consolidate a bulk mass of alloys, compounds, or composites. The bulk mass usually possesses enhanced microstructure without pores, zero grain coarsening, interlocked grain border-lines, cohesive matrix/additive interface, and uniformly dispersed reinforcements [24–26]. Figure 3 shows the fundamental operation of SPS machine.

It can be observed from Fig. 2 that articles on review of HEAs are not as sufficient as it should be taking into consideration the importance of the material to the universal demand, cost, and sustainability of energy. And even though HEAs have good corrosion resistance, some factors such as production technique and elements that constituted the alloy may negatively affect the corrosion properties. Hence, there is the need for deeper insight in the corrosion properties of these alloys processed via SPS. It is clear that SPS technique lacks sufficient research that will fast-track its scalability, affordability, and energy-conservation. So, the need for an in-depth research on the corrosion properties of HEAs is the aim of this study. Therefore, the objective of this work was to critically evaluate recent publications on high-entropy alloys prepared with SPS and their corrosion characteristics. Discussed also is the prospective uses of corrosion-resistant HEAs prepared by SPS together with the challenges encountered in the processing. Research on the corrosion properties of HEAs was motivated by the fact that HEAs are very useful materials with prospective applications in high temperature, high pressure, and high saline environments. These environments are corrosive media which can affect the performance and durability of the materials. Hence, this present work on how HEAs can thrive in these media is not only imperative but timely.

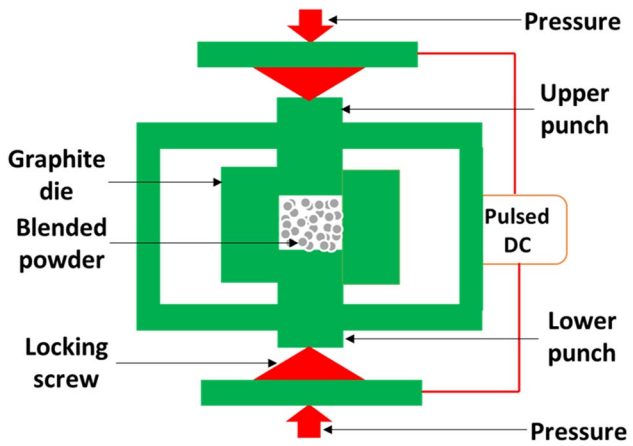

Fig. 3 Schematic diagram of spark plasma sintering technique

2 Corrosion mechanisms in HEAs

The term "corrosion" is the deterioration of substances as a result of their chemical or electrochemical interactions with the ambient [27]. Modes of corrosion will be discussed below.

2.1 Modes of corrosion in HEAs

A) Oxidation: Corrosion can manifest on materials in the form of oxidation. Oxidation is when a material loses electron, or when there is the addition of oxygen to the material. When a material loses electrons to form an ion (cation), the attacking oxygen will gain electron to form oxygen anion. Take for instance, in the oxidation of Zn, the metal loses two (2) electrons to form Zn^{2+} while the O_2 acquires four e^- forming O^{2-} anion. So, in describing corrosion as oxidation process, corrosion manifests in the form of transferring electrons from a metal surface to an oxidizing agent, like oxygen or moisture. This electron transfers will yield positively charged cations on the surface of the metal. The cations are very reactive and can react with atoms or molecules to produce a deposit of oxides, hydroxides, or sulfides. Metals with the deposit of these complexes are said to have corroded. The effect is that the material keeps deteriorating until it fails completely. High-entropy alloys are resistant to oxidative corrosion [28]; however, at elevated temperature, the diffusion of oxygen becomes highly activated. So, its penetration propensity increases. More so, the vibration kinetics of the metal increases and exposes its micro porosity in such a way that diffusion of oxygen triples. One of the characteristics that distinguishes high-temperature materials from other materials is resistance to elevated temperature oxidation. Muller et al. [29] worked on the elevated temperature oxidation mode of the following HEAs: TaMoCrAl, NbMoCrAl, NbMoCrTiAl, and TaMoCrTiAl at 1000 °C in ambient environment. In TaMoCrTiAl HEAs, there was evolution of Al_2O_3, Cr_2O_3, and $CrTaO_4$ protective layers at 1000 °C in air. The oxygen diffusion rate in the HEA slowed from parabolic to quartic rate law as a result of the presence of $CrTaO_4$ in the oxides. For NbMoCrAl and TaMoCrAl HEAs, there was the formation of Al_2O_3, Cr_2O_3, and $CrNbO_4$ protective oxides. However, their oxidation resistance was undermined by the formation of Nb_2O_5 oxide which exhibited anisotropic thermal expansion, activated pore evolution, and scale spallation. Therefore, the availability of Ti provoked the evolution of protec-

tive rutile-type oxide such as $CrTaO_4$ and diminished the concentration of deleterious Nb_2O_5 and Ta_2O_5.

B) Hydrogen embrittlement: Hydrogen embrittlement is a form of corrosion which arises when hydrogen atoms infiltrate into a material, inducing brittleness and crack propagation. Hydrogen atoms can penetrate into a material during production or when in use. Besides the effects mentioned above, H_2 penetration can provoke the following defects: it can lower the tensile strength of a material, it can reduce ductility, it can lower the fatigue strength, and can induce stress corrosion cracking. Hydrogen embrittlement must be tackled headlong to avoid its effects which can cause catastrophic failures. Zhou et al. [30] suggested that hydrogen embrittlement can be removed from materials via heat treatment. Meanwhile, hydrogen embrittlement is more injurious to BCC HEAs than other structural phases of HEAs. Recall that movements of the interstitial atoms are generally more in BCC structures than in FCC structures. That is the major reason why BCC HEAs are developed as hydrogen storage system [31, 32]. It was discovered that hydrogen embrittlement attacks stainless steel more than CrFeMnCoNi HEA, even though hydrogen retention is obtained more in HEAs than in other alloys. After hydrogen charging, HEA's ductility diminished, though only marginally [33]. But when CrFeMnCoNi HEA was reinforced with carbon particles, it manifested more pronounced ductility loss after charging [34].

C) Galvanic corrosion: Galvanic corrosion is experienced in metallic materials when two different metals with wide difference in electrode potentials come in contact with one another, evoking the interchange of electrons between them. Sometimes, galvanic corrosion can set in on a single metallic object when a conducive environment (medium) is present. One end acts like the cathode for deposition of iron (iii) oxides (Fe_2O_3. X_2O) while the other end acts as the anode where dissolution of materials (oxidation) takes place (see Fig. 4). The loss and gain of electrons in the metal surface is cyclic and keeps repeating until the entire material becomes depleted. As a galvanic cell is set up on the metallic surface, the more positively charged material loses electrons [35], becomes oxidized, and goes into the electrolyte while the negatively charged metal gains electrons, becomes reduced, and discharged to the cathode as an oxide. Conditions that stimulate galvanic corrosion include the following: the two materials should have electrical potentials difference, there should be presence of electrolyte (moisture, acid, base, salt, or gas), and the two bodies must have physical contacts [36]. In an experiment involving SPS and annealing of AlCoCrFeNi HEA, there was evolution of B2, BCC, and FCC phases. It was observed that FCC phase was more prone to pitting and some localized corrosion than BCC phase [37]. This may be linked to the evolution of Cr-rich body-centered cubic phase comprising Cr_2O_3 passivation oxide layer that prevented the matrix from further corrosion [38].

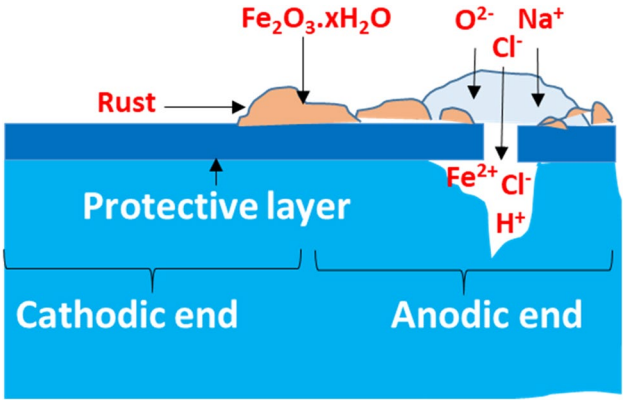

Fig. 4 Schematic diagram of galvanic corrosion

It was opined that breakdown of $CoCr_2O_4$ and $CoFe_2O_4$ oxides may have induced the pitting corrosion [39]. During annealing, increase in annealing temperature increased the corrosion rate because the BCC phase got transformed into sigma phase which led to reduction of corrosion resistance. Galvanic corrosion is experienced around σ-phase and it can be asserted that sigma phase decreases corrosion resistance of HEAs. In another study by Chu et al. [40], $AlCoCrFeNi_{2.1}$ EHEA was produced with SPS. Dual-phased FCC matrix (abundant in iron, cobalt, and chromium) and BCC structure (rich in nickel and aluminum) evolved in the microstructure (Fig. 5). In the electrochemical analysis, it was observed that galvanic corrosion occurred between the two phases with a preferential dissolution of BCC phase. Meanwhile, increasing sintering temperature induced the enlargement of BCC phase (Fig. 5d–f) which evoked a decrease in micro-galvanic corrosion and enhanced the corrosion performance of EHEAs as shown in Fig. 4a–c. So, to improve the corrosion resistance of HEAs against galvanic corrosion, increasing the size and the overall distribution of BCC phase by increasing the sintering temperature and pressure was an effective method. From Fig. 5, it will be noticed that the rate of corrosion of S6 (sample sintered at 1400 °C) was the least (highest impedance to corrosion (Fig. 5b) and least current density (Fig. 5c) while S4 (sample sintered at 1000 °C) had highest corrosion rate (lowest impedance to corrosion (Fig. 5b) and highest current density (Fig. 5c).

In the phase distribution, the FCC phase formed the matrix (green specie) while the BCC phase was the dispersed phase (red specie). When the sintering temperature was raised, it was noticed that the size of BCC phase (phase prone to dissolution) increased, inducing corrosion

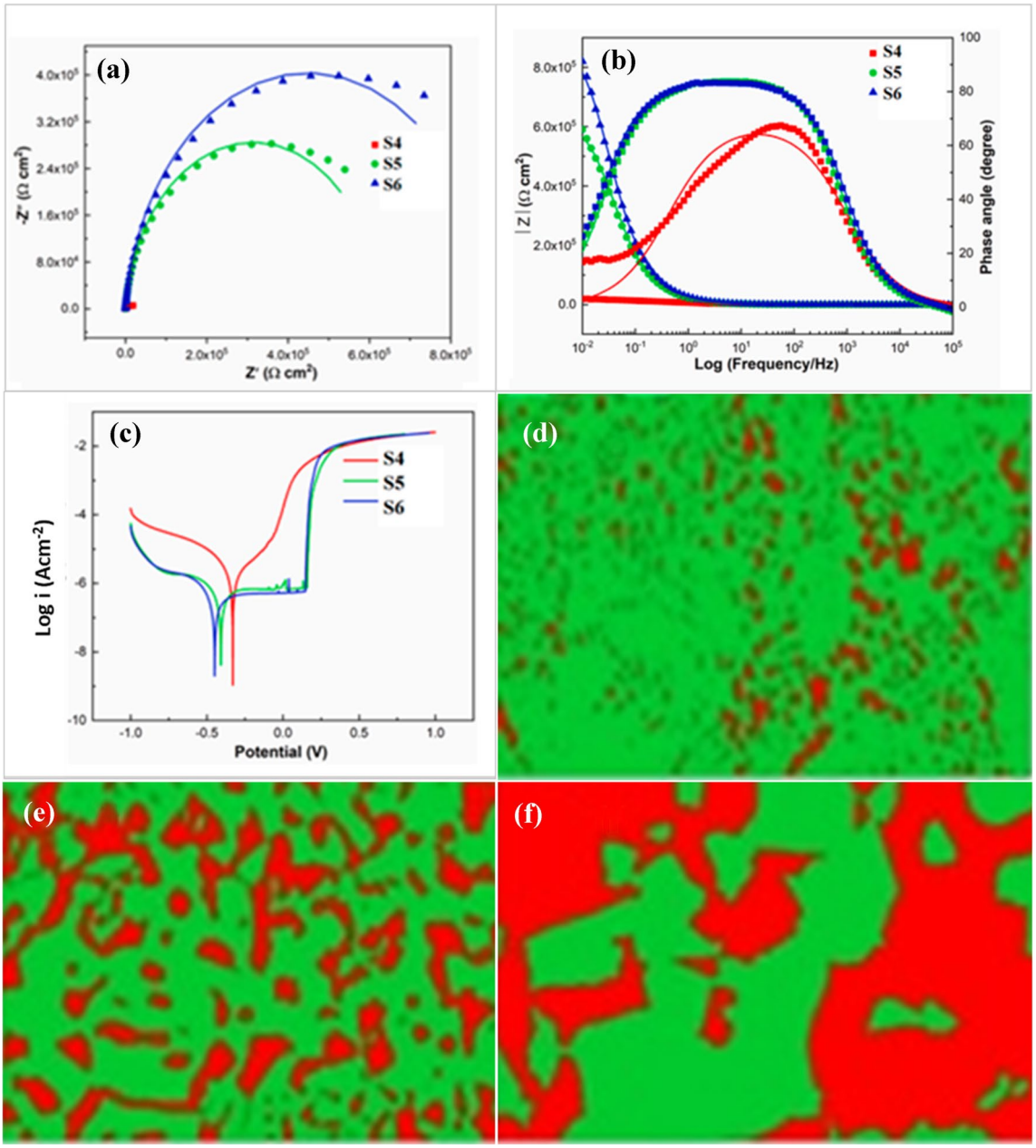

Fig. 5 Plots and phase distribution of HEA processed at (S4 – 1000 °C), (S5 – 1200 °C), and (S6—1400 °C) and all at 35 MPa: (**a**) Nyquist plots showing similar features in capacitive semicircles, (**b**) Bode plots showing high impedance of sample S6, (**c**) potentiodynamic polarization curves, (**d**) phase distribution of S4, (**e**) phase distribution of S5, (**f**) phase distribution of S6 [40]

resistance. It was equally disclosed that higher sintering temperature and pressure increased the densification of the alloy and reduced the pores in the microstructure. The reduced pores enhanced corrosion resistance as pores are usually the nucleation site for material failures [41].

D) Stress corrosion cracking (SCC): This takes place mostly in metals when they are subjected to loading in a corrosive media. Metallic materials fail more when they are stressed heavily in adverse environments. When this sudden crack occurs on stressed components, it is termed SCC. The presence of elements such as chlorine induces the initiation of SCC. In metals like Al alloy or composite, the presence of intermetallic phase favors the occurrence of SCC. In aluminum alloys, SCC is often associated with the presence of intermetallic phases. Stress corrosion cracking can as well affect high-entropy alloys. It has been experienced in NiCoCrFeMn, AlCoCrFeNi, and FeCoNiCrMn HEAs [42, 43]. Here, it is believed that the galvanic corrosion which preferentially

dissolves BCC phase to form pitting corrosion would escalate to SCC when there are favorable conditions of continuous stress and chemical medium. In the presence of these environments, HEAs are more prone to SCC than conventional alloys. The menace of SCC can be controlled in HEAs by incorporating some elements like Cr [44] which enhances the resistance of the alloy against SCC by forming Cr_2O_3 passivation film. Moreover, heat treatment can equally help in decreasing the occurrence of SCC [45].

E) Selective leaching: This is a form of corrosion which takes place in materials including HEAs when one element in the alloy is more readily dissolved than the other elements, inducing its preferential removal. Selective leaching (SL) is an exceptional form of corrosion occurring in between the grains of materials, simply referred to as intergranular corrosion. Its aftermath is the existence of micro voids and cracks at the grain boundaries which subsequently become the point of failure initiation [46]. SL of HEAs is a function of the large number of grain boundaries and the separation of elements at the boundaries. This implies that the control of SL corrosion boils down to the control of the microstructure, especially the control of segregation of the grains in the grain boundaries. Besides causing total failure of the alloy, milder ones induce evolution of void-filled microstructure with subsequent loss of strength and ductility. If materials are not closely watched, their failure from SL is usually abrupt and disastrous, even though the material appears normal and healthy on the surface. Some forms in which SL takes place are as follows: (a) de-zincification—here, HEAs which contains brass (30Zn-70Cu) may readily suffer selective removal of more active zinc atom leaving behind red porous copper [47]. So, in order to control dezincification, the percentage of Zn and Cu must be manipulated so that brass will not evolve. (b) Graphitic corrosion—here, there is preferential leaching of Fe leaving behind porous graphite matrix when HEA containing grey cast (2–4%C, 1–3%Si, Fe) is in an aqueous environment, such as under the soil. The remnant of graphitic corrosion is a porous, rusty, and weak graphitic HEA which can fail suddenly [48]. (c) Dealuminification—this occurs when a HEA that contains bronze (Cu + 8% Al) is placed in a corrosive environment. Here, α-Al is selectively removed from the bronze-containing HEA, leaving behind porous weakened Cu-HEA which is very prone to catastrophic failure [49]. In a research to evaluate the effect of Al element on selective leaching of Al_xCoCrFeNi HEA ($x = 0.2$, 0.6, and 1), Chang et al. [50] observed that SL of $Al_{0.2}$CoCrFeNi high-entropy alloy was a bit higher than that witnessed in the HEA without Al, that is, CoCrFeNi MEA, which evolved a single FCC phase. This was because Al_2O_3 that formed on the surface was porous and weak in protecting the material from SL corrosion, and induced a depletion of more protective Cr_2O_3 and Fe_2O_3 passivation films. Meanwhile, both $Al_{0.6}$CoCrFeNi and $Al_{1.0}$CoCrFeNi evolved BCC + FCC dual phases, and the selective leaching experienced in both was heavier than that observed in single-phase $Al_{0.2}$CoCrFeNi HEA as a result of higher concentration of Al element. Another researcher disclosed that incorporation of Sn on CoCrFeNi HEA is more advantageous in protecting the alloy against SL corrosion than Al or Cu because SnO_2 passive film is more protective and resistant to corrosive elements like Cl^- than Cu_2O and Al_2O_3 passive films [51].

F) Filiform corrosion: This corrosion takes place in HEAs and other materials that contain metals. It manifests as an elongated, thread-like corrosion projection which spreads beneath the surface of the material [52]. Filiform corrosion (FFC) is triggered by chlorides or other corrosive ions, which can infiltrate through an existing protecting oxide film domiciled on the surface of the material. As soon as the corrosive ions get to the metal, they induce localized corrosion at the weakest point of the material's internal structure which is the grain boundaries. As the activity of the localized corrosion perpetuates, it forms filiform corrosion discharges. This filiform product would later get to the surface of the material and form a crack which induce further corrosion. It was suggested that deformation of metal surfaces is the principle initiator of FFC or weak resistance to it. So, surface enhancement through etching improves FFC resistance [53]. When filiform filaments are critically observed, it will be seen that each filament is made up of bifilms, which is a double layer of films that are poorly bonded. Their length is usually the dimension of the bifilms caused by the plastic deformation of the matrix in the direction of rolling. More so, the susceptibility of the deformed surfaces of metals is escalated by the presence of precipitates, second phases, or intermetallic compounds, which is always harder than the matrix of the alloy. These inclusions tend to push their way up and break through the surface during intensive rolling or work hardening if the thickness is very low in the tune of few millimeters [54].

G) Microbiologically influenced corrosion: Microbiologically influenced corrosion (MIC) is initiated by the activities of microorganisms. These microorganisms (bacteria and fungi) are usually attached to the surfaces of the host and develop into biofilms [55]. In the biofilm enclave, the microbes can intermingle with the material surface, setting up environment susceptible to corrosion. Most often, the microbes can secrete corrosive fluids, like acids or sulfides, which are inimical to the

material's corrosion resistance. MIC is very aggressive in the oil and gas industry, water purification amenities, and food processing industry [56]. The outstanding mechanism in which MIC attacks HEAs is through the secretion of biofilms on the surface of the alloy which eventually translate to localized corrosion. Sometimes, the biofilms obstruct oxygen and other reactants from gaining access to the surface of the alloy, hence, setting the arena for anaerobic corrosion [57]. The microbes, as revealed earlier, can secrete H_2S and organic acids which can stimulate pitting corrosion. In other cases, some enzymes can be produced by the microbes which can cause the collapse of the shielding oxide layer of the alloy, thereby exposing the inner part of the alloy to corrosion. It has been recommended that controlling the homogeneity of HEAs so as to forestall localized corrosion is worth it. This is achieved through painstaking selection of the alloying elements and employing robust production route to make sure that there is homogenous dispersion of the constituent elements all over the material. To minimize the menace of MIC, it is encouraged to employ processes that would tolerate zero impurities and defects during production, as they are the nucleating sites of microbe attachment and subsequent localized corrosion [58].

H) Atmospheric corrosion: Atmospheric corrosion (AC) attacks materials exposed to the atmosphere, air, moisture, oxygen, and other corrosive media [59]. AC possesses a great danger to high-entropy alloys because the multiple elements that make up the alloy react to the ambient in various modes. The various reaction modes lead to formation of varying corrosion deposits such as oxides, hydroxides, and sulfides [60]. This implies that the corrosion deposits are not homogenous at all, and this situation exposes the alloy to localized or fatigue corrosion. So, consideration of the presence, the havoc, and effects of AC during the design of HEAs is very imperative. Higher humidity, for instance, influences the rate of AC in high-entropy alloys. More so, presence of acidic oxides, like sulfur dioxide or nitrogen dioxide, also aggravates atmospheric corrosion in HEAs. Microorganisms in the atmosphere equally produces corrosion products that stimulates AC [61]. High temperature and high wind velocity induce the rate of AC. In designing HEAs to control the rate of AC, it is recommended that corrosion-resistant elements, like Cr, Sn, or Al which has the capacity of forming protective film that prevents corrosion, should be incorporated. Application of surface finishing like paints or coating can go a long way in controlling the menace of AC.

I) Erosion corrosion: Erosion corrosion (EC) occurs on metals including HEAs when there is physical removal of shielding film from the topmost layer of the alloy in such a way that the inner layer is exposed and becomes prone to localized corrosion [62], as shown in Fig. 6. The corrosion attacks HEAs mostly because the elements they are made of are not cohesively bonded due to their dissimilarity in size and chemistry. This makes the removal of outer surface of the alloy very easy. When the protective film is removed, localized corrosion pits may strike, and corrosion pits are the failure's nucleating sites [63]. Environments that favor erosion corrosion include marine, industrial, and chemical sites which harbor corrosive impurities, like O_2, N_2, and H_2. The impurities either oxidize or reduce the protective layer of the HEA with subsequent evolution of secondary phases that are more prone to corrosion. More so, these impurities may influence the hydrogen embrittlement of the alloy and induce higher brittleness on it [64]. One other factor that escalates EC is the speed of the corrosive fluid or gas in which the alloy is in contact with, together with its temperature and pH. Effective selection of appropriate elements that can form stable protective film on the top layer of the alloy is one of the ways in ameliorating the menace of EC. Such elements include chromium, molybdenum, tungsten, and niobium. Another technique is by ensuring that the surface finish of the alloy is smooth so that friction which can induce erosion of the surface is controlled. Nair et al. [65] studied the method of ameliorating the cavitation erosion corrosion in materials by preparing $Al_xCoCrFeNi$ ($x=0.1$–3) HEA coating on stainless steel substrate. The whole coatings exhibited more superior resistance to erosion-corrosion than the uncoated substrate. Among the coatings, the equimolar composition provided three times better erosion corrosion resistance than stainless steel. The much better resistance to corrosion of the HEA coating was as a result of the higher fracture toughness, hardness, and work-hardening properties of HEAs. Incidentally,

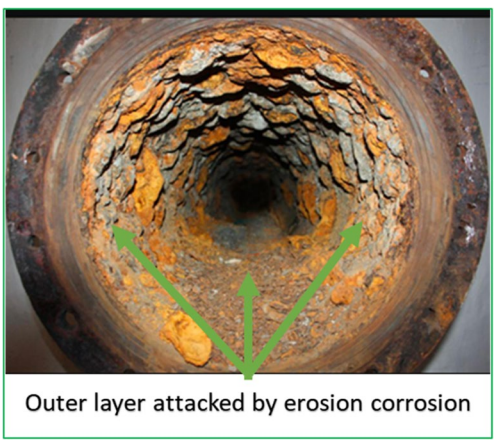

Fig. 6 Erosion corroded metallic component [66]

$Al_3CoCrFeNi$ coating formed porous and unstable passive layer and showed very poor resistance to erosion corrosion. More so, the evolution of secondary sigma and B2 phases depreciated the erosion corrosion resistance of the composite coating. This was because they formed micro galvanic cells and induced chromium-depletion in the microstructure.

J) Crevice corrosion: Crevice corrosion (CC) is a localized corrosion that takes place in a chasm between two surfaces [67]. In HEAs, CC occurs when there is a compositional difference in the alloys thereby forming two surfaces or when there are two surfaces exposed to different environments (Fig. 7). This situation will induce the establishment of corrosive cell where one surface, acting as the anode, corrodes while the other surface acting as the cathode is protected. Crevice corrosion is very dangerous in HEAs because of the large number of elements that form them. The large number of elements creates a heterogonous surface liable to have many sites for crevice corrosion. Having numerous crevice corrosion sites will create a situation where some elements are depleted while others are built up. This abnormality can induce so many other mechanisms of corrosion like pitting, galvanic corrosion, and stress corrosion cracking [68]. Detecting the onset of CC in HEAs is difficult due to the heterogeneity of the surface; hence, the havoc may continue unnoticed until there is sudden catastrophic breakdown of the material [69]. Therefore, it is imperative to take adequate steps to forestall the inception of crevice corrosion. The major step that should be taken to prevent the onset of CC in HEAs is by designing the alloy to consist of very minimal heterogeneity. This is achieved by selecting appropriate elements to be alloyed together with manipulating the production process parameters. Prospective sites for crevices must be handled adequately so as to prevent its initiation and propagation. Existing ones must be reduced to an infinitesimal. Sacrificial anodizing and cathodic protection can equally minimize the ravaging menace of CC. Frequent monitoring and evaluation of the HEA system can be useful in identification of initial signs of crevice corrosion.

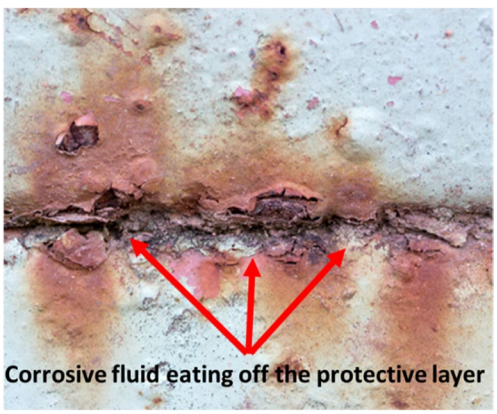

Fig. 7 Crevice corrosion on mild steel plate surface protected with paint [66]

K) Intergranular corrosion: IGC in high-entropy alloys occurs along the grain boundaries of the alloy [70]. IGC has the capacity to initiate premature failure in HEAs because of the multiple grain boundaries therein. This corrosion can be induced in HEAs by the following factors: the constituent of the alloy, the production history, and the alloy's purity. Meanwhile, research suggests that some HEAs are more prone to IGC than others due to the factors listed above among others. Some of the alloys prone to IGC include the Cantor alloy (CoCrFeMnNi), the equiatomic CoCrFeNi alloy, and the $Al_{0.5}CoCrCuFeNi$ HEA [71]. They are very weak to chloride environment. Their susceptibility is attributed to the evolution of microstructure that contains high density of grain boundaries, coupled with the evolution of brittle intermetallics at the grain boundaries. Elements that are prone to brittle intermetallics in the grain boundaries include aluminum, nickel, and chromium [72]. They have the tendency to precipitate out of the alloy and form brittle compounds at the grain boundaries. Most often, the evolved compounds act as stress concentrators where crack initiation and propagation situates. However, element like molybdenum can diminish the susceptibility of HEAs to IGC. The control of IGC in HEAs is very essential in maintaining their robustness and durability.

L) Fretting corrosion: Fretting corrosion (FC) is a wear-assisted corrosion which affects HEAs that are subjected to repeated cyclic loading [73]. FC normally takes place in between two contacting surfaces that are in relative motion. The scratching of the surfaces generates wear debris. The wear debris collects at the gap between the two surfaces and acts like the cathode for corrosion, inducing localized corrosion as the contacting surfaces act as the anode [74]. Hence, loss of electrons (corrosion) in the contacting surfaces sets in. FC can bring about catastrophic damage to HEAs as it can cause colossal loss of materials and subsequent breakdown. There are three major stages of FC in HEAs. Firstly, wear debris and oxides are formed in between the contacting surfaces. These formed substances make the contacting surfaces more susceptible to corrosion. Secondly, the surface layer is forced to breakdown into micro cracks and crevices by the aggregated debris and oxides. The third stage is the propagation of cracks to the whole body of the material [75]. HEAs susceptible to FC include $AlCoCrCuFeNi$ and $FeCoCrNiMo_{0.5}$ HEAs.

Their weakness to FC is attributed to their weakness to friction and wear. More so, they readily form brittle intermetallics (like chromium nitrides or oxides) along their grain boundaries. To enhance HEAs' resistance to FC, it is recommended to incorporate some elements which can form stable protective layers and enhance the mechanical strength of the alloy. Such elements include chromium, niobium, molybdenum, and tungsten. Cr is good at generating protective oxides while Nb and Mo aid in increasing the strength and toughness of the alloy; and W is well known in increasing the wear resistance of HE alloys.

3 Enhancement of corrosion resistance during the synthesis of HEAs

I) During SPS of high-entropy alloys, the alloying of large number of different elements can lead to the evolution of numerous corrosion products that can subsequently aggregate to form a shielding film which can protect the alloy against corrosion. Oxide layers of Cr, Al, or Si, for instance, are readily formed during the alloying of HEAs. This oxide film can consist of one or combination of two or more of those elements existing in crystalline or amorphous structure. Their formation can aid in prevention of further corrosion through obstructing the diffusion of O_2 and H_2O into the substrate. Some other protective corrosion products formed by the alloying elements of HEAs include hydroxides and carbides. Their formation can prevent further oxidation of the inner materials. Muangtong et al. [51] studied the corrosion characteristics of CoCrFeNi-x (x = Cu, Al, Sn) HEA in Cl^- medium. Among the three HEAs developed and tested, it was CoCrFeNiSn that formed the most stable Cr_2O_3 and SnO_2 films on the surface of the sample which prevented further corrosion of the alloy. Figure 8 shows backscattered scanning electron microscope (BSEM) images of the HEA samples immersed in NaCl medium. From the figures, it can be seen that it was the microstructure of CoCrFeNiSn (Fig. 8d) that showed highest resistance to corrosion as a result of the evolution of more stable oxide layers of Cr_2O_3 and SnO_2. This result confirms that CoCrFeNiSn is useful adverse environment, like in marine applications. Other HEA samples were not as resistant to corrosion as CoCrFeNiSn as evidenced by their microstructures in Fig. 8b and c. Their poor resistance to corrosion was attributed to the weaknesses of Al_2O_3 and Cu_2O protective films to chloride ions.

II) The non-similarity in the composition of SPSed HEAs usually induces a uniform dispersion of cor-

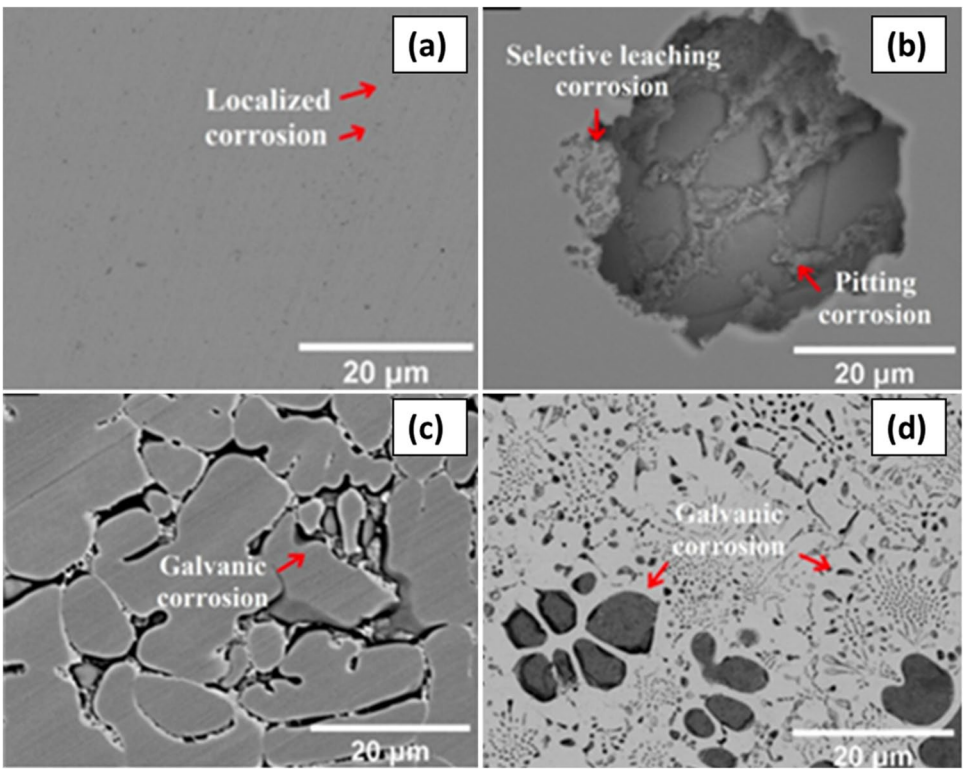

Fig. 8 BSEM images of HEAs immersed in 0.6 M NaCl: (**a**) CoCrFeNi, (**b**) CoCrFeNiAl, (**c**) CoCrFeNiCu, and (**d**) CoCrFeNiSn [51]

rosion products, which leads to improvement against localized corrosion of SPSed HEAs. This can be possible through the evolution of a passivation layer which obstructs further corrosion. Note that in HEAs, the evolution of a passivation film is stimulated by the existence of manifold elements which form complex oxides, sulfides, or carbides on the top layer of the alloy. This passivation film prevents the filtration of corrosive compounds, ions, or molecules into the metal's outer and sub-surfaces, thus shielding the material from further corrosion. So, the uniform distribution of corrosion products in HEAs can induce the evolution of a homogeneous surface, decreasing their susceptibility to stress corrosion cracking, fretting corrosion, crevice, and other forms of localized corrosion [76].

III) The existence of equiatomic or near-equiatomic elements in the place of one primary element in HEAs can promote more stable corrosion-resistant surface. This is made possible by altering the surface reactivity and the chemistry of the passivation layer. More so, synergistic effects of the alloying elements can promote the formation of new phases or stabilization of the passivation layer which improves the resistance to corrosion of the alloy. Note that the stabilization of chromium oxide in the passivation layer of the high-entropy alloy is usually the principal cause for the superior corrosion characteristics of Cr-containing HEAs. A study was conducted on the corrosion characteristics of NiCoCr, NiCoFe, NiCoCrFe, and NiCo alloys in 0.1 M HCl and 0.1 M NaCl media. It was observed that a solid solution of chromium in the high-entropy alloys helped in improving the corrosion resistance of the alloy.

The stabilization of Cr_2O_3/$Cr(OH)_3$ in the passivation layer was the principal factor that contributed to the improved corrosion resistance. More so, a small incorporation of molybdenum, tungsten, and titanium in high-entropy alloys can help to transform [OH] to [O] in the passivation layer and escalate the quantity of Cr_2O_3 in the passive film, thereby, inducing the strength and fortification of the passivation layer of the alloy [77].

IV) Incorporation of Al into HEAs

Besides contributing to the decrease in the density of HEAs, incorporating Al into high-entropy alloys aids in increasing the strength and corrosion characteristics of the bulk material [78–81]. HEAs which contain Al normally generate passivation layer of Al_2O_3; so, they are considered to be highly resistant to corrosion as the passive film shields them from further corrosion. Therefore, incorporating Al into HEAs enhances the shielding of the passive film as observed in a research of Ni-based HEAs [82], but Al is not as superior as some other elements in protecting alloys from galvanic corrosion. Al is usually preferentially dissolved in solution in the place of iron, cobalt, chromium, and nickel counterparts when in contact with corrosive medium. Corrosion characteristics of $Al_xCoCrFeNi$ ($x = 0$, 0.25, 0.5, 1) HEAs was investigated by Shi et al. [83] via immersing them into numerous corrosive media. By raising the Al content in $Al_xCoCrFeNi$ HEAs, there was a corresponding rise in the volume fractions of the aluminum-nickel-rich film with an evolution of body-centered cubic phase bereft of chromium. This made the alloy susceptible to chloride attack, which implies that Al content must be kept low. In another study, incorporation of Al element induced BCC phase formation. The authors discovered that when the content of Al increased, the microstructural configuration drifted from single face-centered cubic phase to double face-centered cubic and body-centered cubic phases [84]. Further increment of Al led to depletion of FCC, remaining single phase BCC which is more prone to corrosion as observed also in $Al_xCrFe_{1.5}MnNi_{0.5}$ HEAs [85]. It is on record that BCC phase is more susceptible to corrosion than FCC phase [86].

V) Incorporation of Cr in HEAs

The remarkable resistance to corrosion of stainless steel is linked to the passivation layer generated on its surface by Cr oxide/hydroxide [87]. Research has shown that the percentage of Cr that can generate adequate passivation film should be greater than or equal to 12 at% [88]. Meanwhile, in HEAs, Cr equally helps in improving their resistance to corrosion as evidenced in many researches. A work by Chai et al. [89] was aimed at investigating the effect of chromium on the electrochemical properties of $FeCoNiCr_x$ HEA having value of x as follows: $x = 0$, 0.5, 1.0. The HEAs was composed of face-centered cubic phase after the fabrication. They were dipped into 0.5 M hydrogen sulfate acid and 3.5 wt.% sodium chloride solution. It was observed that $FeCoNiCr_{0.5}$ HEA maintained a columnar cell shape. However, the passivation region as well as polarization potential of $FeCoNiCr_{0.5}$ HEA rose considerably in the two media. However, when the Cr content was raised very high, there was evolution of dendrites with chromium separation in the interdendritic portions which were readily dissolved by Cl^- ions, escalating pitting corrosion; this trend was equally observed by Tsau eta al. [90]. This implies that an adequate Cr content improves the corrosion resistance of HEAs in sulfuric acid and chloride ion media. So, Cr contributes

to the stabilization of passive film which increases the resistance to pitting corrosion, but there is caveat here. Incorporation of excess Cr into HEAs stimulates aggressive pitting corrosion as a consequence of Cr segregation which takes place at the interdendritic regions.

VI) Addition of Ni in HEA

Ni is a renowned element for impacting excellent mechanical, oxidation, and corrosion properties on alloys and composites [91, 92]. Ni-based alloys are resistant to corrosion in acid-induced and stress-induced corrosions as it is witnessed in the petroleum and petrochemicals, electrical, and electronic industries [93]. The adequate volume weight of nickel in high-entropy alloys surpasses its weight in stainless steel. However, its weight in superalloys still surpasses its weight in HEAs. Nevertheless, the presence of nickel provides a good support system in enhancing HEAs' resistance to corrosion [94]. The research of Qiu et al. [95] was based on corrosion behavior of high-entropy alloys. Their case study was on $Al_2CrFeCoCuTiNi_x$ HEA with the values of x as follows: $x = 0$, 0.5, 1, 1.5, 2.0. The test media included 1 M sodium hydroxide and 3.5 wt.% sodium chloride solution. FCC and BCC dual-phased structure was formed in the $Al_2CrFeCoCuTiNix$ HEA, which implied that the presence of Ni could not alter the microstructural composition. Results showed that the corrosion resistance of $Al_2CrFeCoCuTiNi_x$ high-entropy alloy started increasing as the volume of Ni was raised but later reduced with rise in Ni volume in both alkali and salt media (Fig. 9a and b). The $Al_2CrFeCoCuTiNi$ alloy possessed the least corrosion current density as a result of high densified microstructure. In HEAs' passive film, Ni can exist in the form of oxides, hydroxides, or in metallic state. It is difficult to differentiate Ni from other elements using XRD spectrometry in stainless steel because Ni content is very low [96]. This makes it difficult to attribute the electrochemical behavior of 304 stainless steel to Ni. But in HEAs, the content of Ni is escalated and a lot of research has attributed their corrosion resistant to Ni content in the metallic state at the metal/oxide interface through reduction or the dissolution of the oxide films [97].

VII) Incorporation of Ti in HEA

The microstructure of HEAs containing Ti is rather complicated as intermetallic phases usually precipitate during their formation [98, 99]. It was reported that when Ti concentration increased in FeCoCrAlNiTix ($x = 0.5$, 1, 1.5, 2) HEAs, Ti_2Ni intermetallic developed [99]. Likewise, when the concentration of Ti escalated in $Al_{0.3}CrFe_{1.5}MnNi_{0.5}Ti_{x,}$ for $x > 0.5$

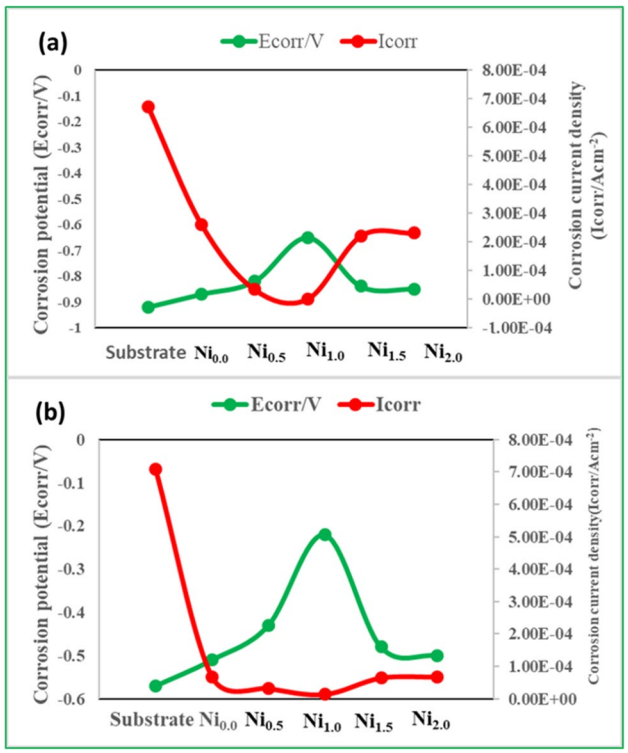

Fig. 9 Corrosion characteristics of $Al_2CrFeCoCuTiNix$ with various content of Ni in (**a**) 1 M NaOH, and (**b**) 3.5 wt.% NaCl solutions (1wt.%Ni possessed the best corrosion characteristics), adapted from [95]

HEAs, there occurred the precipitation of CrNiFe and Cr_9Al_{17} intermetallics [100].

In another study [101], it was observed that when a titanium to aluminum ratio increased in $Al_{2-x}CoCrFeNiTi_x$ high-entropy alloy, there occurred the evolution of Laves and body-centered phases which enhanced the refinement of the microstructure. It was observed that $Al_{1.2}CoCrFeNiTi_{0.8}$ HEAs underwent dendritic crystallization. Body-centered phase was formed which comprised the dendritic region rich in Al-Ni–Ti structure, with iron-chromium-rich precipitates. The interdendritic spaces comprised of iron and chromium metallic inclusions. This implied that incorporation of titanium stimulated the formation of complex micro-structured HEAs where the intermetallic precipitate was the target area for aggressive corrosion. However, in spite of complex microstructure, the $Al_{2-x}CoCrFeNiTi_x$ HEAs with Ti possessed more noble passive layer and superior breakdown potential than $Al_2CoCrFeNi$ HEA without Ti in 3.5 wt.% sodium chloride medium. The superior corrosion characteristics were linked to presence of TiO_2 in the passivation layer of HEAs containing Ti, which was good at enhancing resistance to pitting

corrosion. Moreover, the Ti atom present in the passive film could not be oxidized. This prevented the easy translocation of point defects and helped in stabilizing the passivation layer. Meanwhile, the study conducted by Öztürk et al. [102] gave the impression that incorporating Ti into HEAs degrades its resistance to corrosion as can be seen in Fig. 10. Ti-free CoCuFeMnNi HEAs generated a homogeneous microstructure as a result of positive mixing enthalpy of Cu present in the alloy. However, when Ti was introduced, there occurred an evolution of Ti–rich interdendritic regions. As can be seen in the polarization curve in Fig. 10a, the resistance to corrosion of CoCuFeNiMnTix HEAs reduced with rise in titanium content. The corrosion potential (Ecorr) (Fig. 10b) and current density (Icorr) (Fig. 10b) of the Ti-free HEAs were the biggest and smallest, respectively, when compared with the Ti-containing HEAs, confirming that Ti addition produced poor corrosion result. From Fig. 10c, it could be seen that the rate of corrosion of Ti-free alloy was lower than the Ti-containing HEAs. However, it was noticed that pitting corrosion was the mode of corrosion in the Ti-free CoCuFeNiMn alloy, but after the formation of Ti–rich interdendritic zones as a result of Ti addition, the corrosion turned to galvanic mode.

VIII) Addition of Cu in HEA

Traces of Cu in stainless steel enhanced the corrosion properties of the composite. However, incorporation of Cu in HEAs induces segregation of elements in the interdendritic portions and grain boundaries because Cu has very low bonding with other elements [103]. It was observed that incorporating Cu into FeCoNiCr-based HEAs stabilized FCC phase in the alloy. However, its excess stimulated elemental separation in the interdendritic area which generated a potential difference among the dendritic and the interdendritic regions, hence paving way for galvanic corrosion. Electrochemical characteristics of eight kinds of CuCrFeNiMn HEAs immersed in 1 M hydrogen sulfate acid were conducted by Ren et al. [104]. The incorporation of Cu in the alloy helped in the stabilization of FCC phase. But when the content of Cu was increased, there occurred segregation of elements in the interdendritic regions. $CuCr_2Fe_2Ni_2Mn_2$ HEAs exhibited the best corrosion properties among the researched CuCrFeNiMn HEAs. This was because of homogenous dispersion

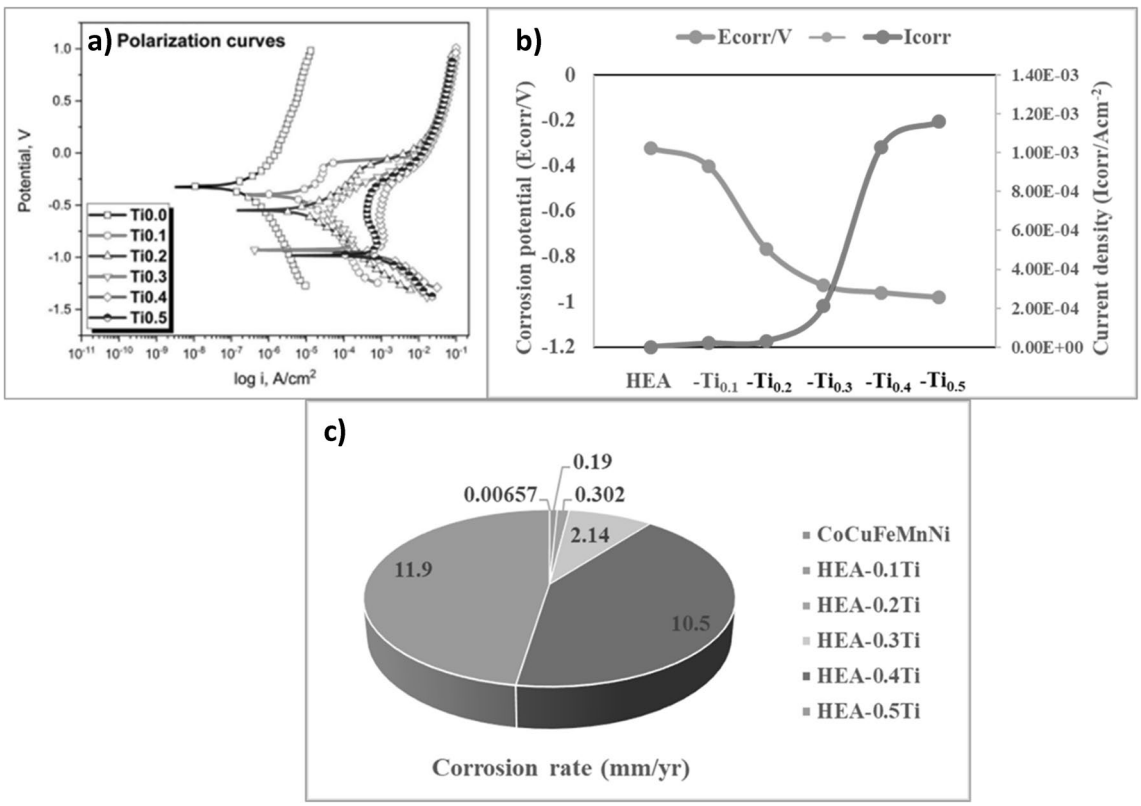

Fig. 10 Corrosion \characteristics of CoCuFeMnNi-Tix HEAs in 3.5 wt.% sodium chloride (**a**) potentiodynamic polarization curves, (b) Ecorr and Icorr curves, and (**c**) corrosion rate chart [102]

of elements together with formation of single FCC microstructure.

Nene et al. [105] investigated corrosion characteristics of HEAs containing Cu. It was observed that pitting corrosion was the major corrosion ravaging $Fe_{38.5}Mn_{20}Co_{20}Cr_{15}Si_5Cu_{1.5}$ HEAs immersed in 3.5 wt.% sodium chloride medium. Copper-rich region was selectively dissolved by Cl^- ions, culminating to total annihilation of the Cu-rich phase in the alloy. Furthermore, when small quantity of Cu was incorporated into $Mn_{1.05}Fe_{0.9}P_{0.5}Si_{0.5}Cu_x$ ($x = 0, 0.05, 0.1, 0.15$) HEAs, it increased its corrosion potential and current density initially and decreased them later on. This was because pure copper phase was precipitated at the grain boundaries and this prevented smooth transfer of corrosive ions [106]. So, the incorporation of small content of Cu into HEAs helps in the stabilization of FCC phase, thereby improving the corrosion resistance. But when added in excess, it stimulates separation of elements at the grain boundaries and interdendritic areas, promoting aggressive and localized corrosion in HEAs.

4 Prospects and challenges of producing corrosion resistant HEAs with SPS

4.1 Prospects of spark plasma-sintered corrosion-resistant HEAs

Spark plasma sintering is renowned for improving the mechanical, corrosion, and microstructural properties of metals, alloys, and composites [24, 107–109]. This is because it stimulates the evolution of highly purified and densified microstructure with refined grains, zero grain growth with minimal formation of detrimental intermetallic compounds [13, 110–112]. These attributes make it one of the best choices in the development of corrosion resistant HEAs. This can be explained by noting that the major causes of corrosion in HEAs include segregation of alloying elements in the grain boundaries and interdendritic regions, weak grain boundaries, non-homogenous microstructures, and presence of micro pores, precipitates, and point defects [113–118]. Interestingly, these defects are specially controlled by SPS. Hence, HEAs produced by SPS are corrosion resistant and can be usefully employed in petroleum and petrochemical industries for the production of oil drilling downhole tools such as drill bit, logging tools, and perforating guns (Fig. 11) which work inside the earth crust with crust's inherent high temperature, high pressure, and highly corrosive. Some of the HEAs used in the production of offshore oil exploration tools include CoCrMo-based, NiCrMoW-based, and TiAlVNb-based HEAs with optimum strength-to-weight ratio, excellent corrosion resistance, high creep resistance, and high thermal stability.

SPS has the propensity of generating highly densified HEAs with prospective application in the production of corrosion-resistant coatings for high-temperature alloys. It energizes the production of coatings with a high level of adhesion to the substrate with zero porosity. This is essential for their efficient and effective performance in development of aerospace engine nozzles and turbines. Moreover, the capacity to put into control the microstructural configuration and composition of the HEAs during SPS permits for the development of coatings/bulks with tailored properties that can be used in high-temperature applications like in nuclear reactors, petroleum distillation reactors, and chemical reactors. The high densification of SPSed HEAs is useful in resisting high-temperature oxidation [120] because high-temperature degradation initiates mostly from weak grain boundaries, micro pores, and impure sites. So, since SPS is noted for producing bulk materials devoid of pores and impurities, its products can withstand high temperatures [121, 122].

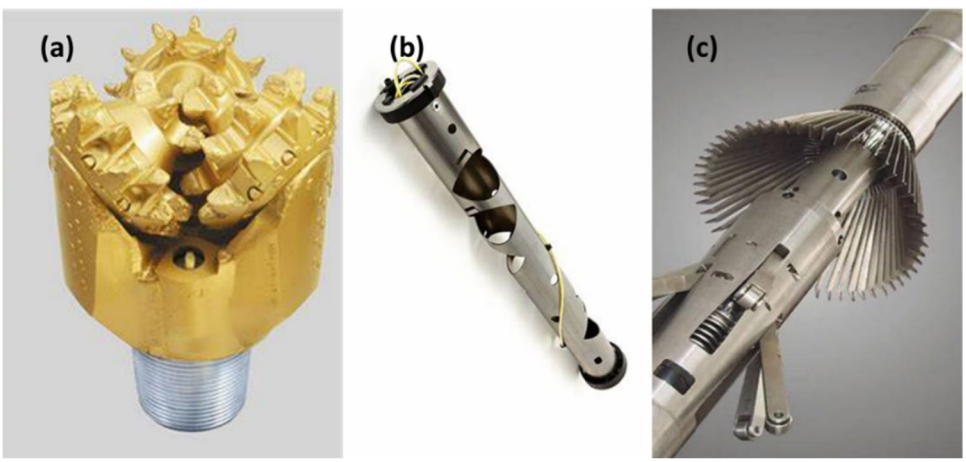

Fig. 11 Petroleum drilling tools: (**a**) oil rig drill bit; (**b**) perforating gun; (**c**) multi-finger caliper logging tool [119]

Corrosion-resistant HEAs produced via SPS possess excellent chemical compositions required for the production of energy storage and conversion devices (Fig. 12). Through manipulation and optimization of the sintering parameters [123, 124], the chemical composition of the microstructure can be tailored to a desired configuration required for specialized energy storage applications. After optimized production of the alloy, it would possess high electrical conductivity, excellent strength, and good thermal stability requisite for energy storage [125–127]. The properties above are required for effective performance in hydrogen storage, electrodes, separators, and electrolytes for batteries. Moreover, the capacity of SPS to modify the configuration of the HEAs makes it fit for the development of supercapacitor with high power density, electrochemical sensors, and electrodes with high energy density and many other electrochemical devices. Some HEAs being projected for energy storage include TiZrHfMoNb (solar energy) [128], and TiVZrNbHf, FeMnCrTiVZr, TiNbVZrHf, and TiNbVZr (H_2 energy) [129–132].

Furthermore, corrosion-resistant HEAs produced via SPS possess excellent mechanical and biocompatible properties requisite for medical implants, pharmaceutical, and biomedical applications [133–135]. This is because SPS technique is specialized in the fabrication of alloys with intricate configurations which cannot be developed easily with other techniques. Such properties bequeathed by SPS technique include high strength and toughness that are requisite for the development of hip, tooth, and knee bone implants [80, 110, 123, 136]. High corrosion-resistant HEAs are quite necessary in the biomedical implants because the body fluids are corrosive and readily present to dissolve any non-corrosion-resistant implants.

But chloride ions as well as other corrosive agents in the body would have little dissolution effects on resistant implants because of the passive film which shields the implant [137–139]. Interestingly, HEA implants developed via SPS possess high resistance to fatigue [140]. Recall that dental implants and hip implants (Fig. 13a and b) are always subjected to cyclic loading. So, with adequate resistance to the fatigue stress, they cannot fail easily. Some HEAs with potential properties for implants include TiZrNbTaMo [141], TiZrNbTaFe [133], and TiZrHfNbTa [142].

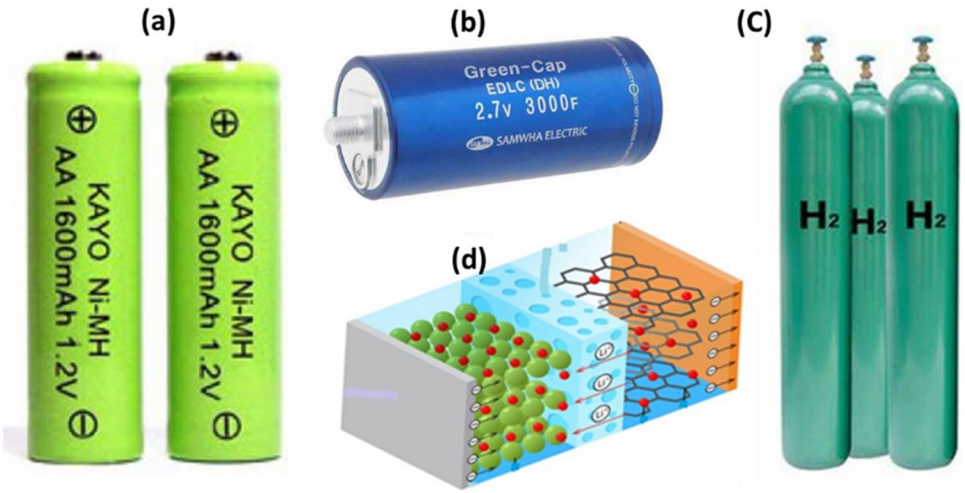

Fig. 12 Energy storage devices: (**a**) primary cell battery; (**b**) supercapacitor; (**c**) hydrogen energy storage; (**d**) Li^+ ion battery

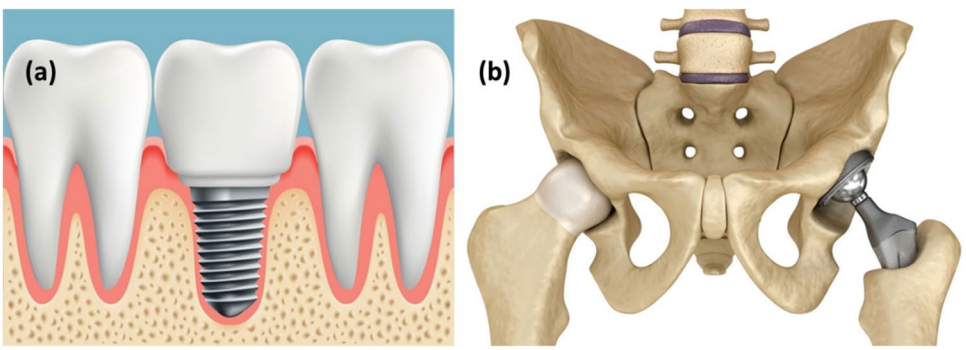

Fig. 13 Medical implants: (**a**) tooth implant; (**b**) hip implant [143]

4.2 Challenges of corrosion-resistant HEAs produced with SPS

I) Brittleness: One of the major causes of brittleness in HEAs is their high lattice distortion which creates imperfections in the crystal structure of the alloy [144]. These imperfections are usually induced during the fabrication of the alloy which stimulates a high level of internal stress. Presence of internal stress, of course, evokes premature cracking and failure. Even though HEAs are known to be very strong and have high resistance to corrosion, they have been observed to have the high brittleness. This challenge makes them hard to be worked with because they readily fracture or crack when subjected to a reasonable stress. To tackle this challenge, elements like Al, Mg, Mn, Si, or Cu should be incorporated into the HEA in order to reduce the brittleness [145]. Alternatively, elements like Cr or W should be added to increase the strength of the HEA and diminish its brittleness. More so, heat treatment can modify the grain structure and improve its strength and ductility [146].

II) Complexity in the microstructure: The complex nature of HEAs' microstructure can make prediction of their properties difficult. This is true because they have high level of chemical disorder which induces irregular and unpredictable arrangement of the atoms in lattice structure. So, modeling this type of alloy with the aim of predicting their properties at some given conditions is quite difficult due to the high level disorder. Again, the complexity of the microstructure leads to heterogeneous grain boundaries with dissimilar characteristics. Hence, the prediction of such material with non-uniform grain boundary properties is almost impossible [147, 148]. The solution to this challenge is further research on microstructural properties of HEAs.

III) Cost of SPS production technique: In comparison with other traditional fabrication techniques of metals and their alloys, like casting and machining, the cost of producing HEAs with SPS is higher. Stir casting is simpler and less expensive. This makes SPS products more expensive to acquire [149]. Further research on this technique is the possible solution to reduce the cost and increase its commercial value.

IV) Limited formability: one other outstanding challenge of HEAs in general is their difficulty in being shaped or formed into a desired configuration. This is because of their high yield strength, low ductility, and susceptibility to cracking at slightly increased loading [150, 151]. So, production of complex shapes like teeth or hip implants with HEAs may be very difficult, if not impossible [12]. To tackle this issue, incorporation of elements like Al, Cr, Mg, or Mn to boost their ductility, fracture toughness, and most other mechanical properties is encouraged.

V) Poor weldability: HEAs are not easily joined with other materials via conventional welding method. This dwarfs their possible application on where different parts need to be joined together with traditional welding. The poor weldability of HEAs is as a result of high level of chemical disorder in them which invokes poor cohesion at the grain boundaries which induces cracks after welding [152]. More so, the high yield strength of HEAs makes it almost impossible to attain to the level of heat that can melt and fuse them together. More advanced welding technique needs to be developed to be able to join HEAs together for some applications [153].

VI) Poor biocompatibility: It has been reported that some HEAs have shown signs of cytotoxicity. This implies that they can be injurious to the body cells or even exterminate them. Such HEAs containing Ni and Mn ions show some elements of cytotoxicity [154–156], and can be injurious when they are used as implants. When such HEAs is employed for implants or prosthetics, they result in serious crisis in the body. Some other HEAs have shown some inflammatory reactions to patients that received them as implants causing severe pains and uneasiness. To tackle this challenge, further research on innocuous elements and ions suitable for medical implants is required.

5 Conclusion and recommendation

I) Brittleness is a major challenge of corrosion-resistant HEAs prepared by SPS. So, to ameliorate this challenge, it is recommended that HEAs should contain Al, Mg, Mn, Si, or Cu to reduce the brittleness; alternatively, elements like Cr or W should be incorporated to increase their strength. Sometimes, heat treatment can reduce brittleness in HEAs.

II) Modeling to predict the characteristics of HEAs is very difficult if not almost impossible due to their high level of disorder during formation. So, further research is recommended in the modeling and simulation of HEAs in order to predict precisely their properties at any given condition.

III) HEAs in general are very difficult to form into complex shapes and structures because of their high yield strength. Hence, incorporation of elements like Al, Cr, Mg, or Mn to boost their ductility, and fracture toughness is recommended so as to improve their applications in the production of complex shapes.

IV) Corrosion-resistant HEAs containing Ni or Mn ions is cytotoxic to the body. So, this kind of elements

should not be incorporated into HEAs for biomedical implants.

V) Corrosion types that ravage HEAs are manifold. It is recommended that carefully selecting corrosion-resistant elements and optimizing the SPS parameters will go a long way into developing robust HEAs for industrial, medical, and household applications.

VI) Corrosion-resistant HEAs prepared with SPS have potential applications in medical and biomedical implants because of their biocompatibility and high resistance to corrosion; in petroleum exploration because of their ability to withstand high temperature, pressure, and saline environments; and in energy storage devices because of their high power and energy densities.

Funding Open access funding provided by University of Johannesburg. The authors acknowledge the financial support of University of Johannesburg and National Research Fund (NRF), South Africa.

Declarations

Conflict of interest The authors declare no competing interests.

References

1. Yeh A et al (2015) Developing new type of high temperature alloys–high entropy superalloys. Int J Metall Mater Eng 1(107):1–4
2. Sims ZC et al (2017) High performance aluminum–cerium alloys for high-temperature applications. Mater Horiz 4(6):1070–1078
3. Bush R, Brice C (2012) Elevated temperature characterization of electron beam freeform fabricated Ti–6Al–4V and dispersion strengthened Ti–8Al–1Er. Mater Sci Eng, A 554:12–21
4. Troparevsky MC, Morris JR, Kent PR, Lupini AR, Stocks GM (2015) Criteria for predicting the formation of single-phase high-entropy alloys. Phys Rev X 5(1):011041
5. Fergachi O et al (2019) Corrosion inhibition of ordinary steel in 5.0 M HCl medium by benzimidazole derivatives: electrochemical, UV–visible spectrometry, and DFT calculations. J Bio-and Tribo-Corrosion 5:1–13
6. Zeng Y et al (2020) Ultra-high-temperature ablation behavior of SiC–ZrC–TiC modified carbon/carbon composites fabricated via reactive melt infiltration. J Eur Ceram Soc 40(3):651–659
7. Tillmann W, Ulitzka T, Wojarski L, Manka M, Ulitzka H, Wagstyl D (2020) Development of high entropy alloys for brazing applications. Welding World 64:201–208
8. Zhou W et al (2017) Deformation stimulated precipitation of a single-phase CoCrFeMnNi high entropy alloy. Intermetallics 85:90–97
9. Cantor B, Chang I, Knight P, Vincent A (2004) Microstructural development in equiatomic multicomponent alloys. Mater Sci Eng, A 375:213–218
10. Yeh JW et al (2004) Nanostructured high-entropy alloys with multiple principal elements: novel alloy design concepts and outcomes. Adv Eng Mater 6(5):299–303
11. Yao C, Huang J, Zhang P, Wu Y, Xu B (2009) Tempering softening of overlapping zones during multi-track laser quenching for carbon steel and alloy steel. Trans Mater Heat Treatment 30(5):131–135
12. Miracle DB, Senkov ON (2017) A critical review of high entropy alloys and related concepts. Acta Mater 122:448–511
13. Ujah CO, Popoola PA, Popoola OM, Afolabi EA, Orji UO (2022) Investigating the nanomechanical and thermal characteristics of Ti20-Al20-V20-Fe20-Ni20 HEA developed via SPS for high energy applications. Metallurg Res Technol 119(6):616
14. Bondesgaard M, Broge NLN, Mamakhel A, Bremholm M, Iversen BB (2019) General solvothermal synthesis method for complete solubility range bimetallic and high-entropy alloy nanocatalysts. Adv Func Mater 29(50):1905933
15. Liu M, Zhang Z, Okejiri F, Yang S, Zhou S, Dai S (2019) Entropy-maximized synthesis of multimetallic nanoparticle catalysts via a ultrasonication-assisted wet chemistry method under ambient conditions. Adv Mater Interfaces 6(7):1900015
16. Yao Y et al (2018) Carbothermal shock synthesis of high-entropy-alloy nanoparticles. Science 359(6383):1489–1494
17. Gao S et al (2020) Synthesis of high-entropy alloy nanoparticles on supports by the fast moving bed pyrolysis. Nat Commun 11(1):2016
18. Liu R, Wang W, Chen H, Lu Z, Zhao W, Zhang T (2019) Densification of pure magnesium by spark plasma sintering-discussion of sintering mechanism. Adv Powder Technol 30(11):2649–2658
19. Cai B et al (2021) Spark plasma sintered Bi-Sb-Te alloys derived from ingot scrap: maximizing thermoelectric performance by tailoring their composition and optimizing sintering time. Nano Energy 85:106040
20. Olevsky EA, Bradbury WL, Haines CD, Martin DG, Kapoor D (2012) Fundamental aspects of spark plasma sintering: I. Experimental analysis of scalability. J Am Ceram Soc 95(8):2406–2413
21. Jiang Q et al (2020) Enhanced magnetic properties and improved corrosion performance of nanocrystalline Pr-Nd-Y-Fe-B spark plasma sintered magnets. J Mater Sci Technol 58:138–144
22. Fu Z, Chen W, Xiao H, Zhou L, Zhu D, Yang S (2013) Fabrication and properties of nanocrystalline Co0. 5FeNiCrTi0. 5 high entropy alloy by MA–SPS technique. Mater Design 44:535–539
23. Moazzen P, Toroghinejad MR, Cavaliere P (2021) Effect of Iron content on the microstructure evolution, mechanical properties and wear resistance of FeXCoCrNi high-entropy alloy system produced via MA-SPS. J Alloy Compd 870:159410
24. Oliver UC, Sunday AV, Christain EI-EI, Elizabeth MM (2021) Spark plasma sintering of aluminium composites—a review. Int J Adv Manuf Technol 112:1819–1839
25. Thomson K, Jiang D, Yao W, Ritchie R, Mukherjee A (2012) Characterization and mechanical testing of alumina-based nanocomposites reinforced with niobium and/or carbon nanotubes fabricated by spark plasma sintering. Acta Mater 60(2):622–632

26. Ujah CO, Kallon DVV, Aigbodion VS (2022) Overview of electricity transmission conductors: challenges and remedies. Materials 15(22):8094
27. Chatterjee U, Bose SK, Roy SK (2001) Environmental degradation of metals: corrosion technology series/14. CRC Press
28. Quiambao KF et al (2019) Passivation of a corrosion resistant high entropy alloy in non-oxidizing sulfate solutions. Acta Mater 164:362–376
29. Müller F et al (2019) On the oxidation mechanism of refractory high entropy alloys. Corros Sci 159:108161
30. Zhou S et al (2019) High entropy alloy: a promising matrix for high-performance tungsten heavy alloys. J Alloy Compd 777:1184–1190
31. Pickering EJ, Carruthers AW, Barron PJ, Middleburgh SC, Armstrong DE, Gandy AS (2021) High-entropy alloys for advanced nuclear applications. Entropy 23(1):98
32. Shen H et al (2020) Compositional dependence of hydrogenation performance of Ti-Zr-Hf-Mo-Nb high-entropy alloys for hydrogen/tritium storage. J Mater Sci Technol 55:116–125
33. Zhao Y et al (2017) Resistance of CoCrFeMnNi high-entropy alloy to gaseous hydrogen embrittlement. Scripta Mater 135:54–58
34. Luo H, Li Z, Lu W, Ponge D, Raabe D (2018) Hydrogen embrittlement of an interstitial equimolar high-entropy alloy. Corros Sci 136:403–408
35. Yang D, Mei H, Wang L (2019) Corrosion measurement of the atmospheric environment using galvanic cell sensors. Sensors 19(2):331
36. Lacina K, Sopoušek J, Skládal P, Vanýsek P (2018) Boosting of the output voltage of a galvanic cell. Electrochim Acta 282:331–335
37. Zhou P, Xiao D, Yuan T (2020) Microstructure, mechanical and corrosion properties of AlCoCrFeNi high-entropy alloy prepared by spark plasma sintering. Acta Metallurgica Sinica (English Letters) 33:937–946
38. Xiao D et al (2017) Microstructure, mechanical and corrosion behaviors of AlCoCuFeNi-(Cr, Ti) high entropy alloys. Mater Des 116:438–447
39. Zhang B, Zhang Y, Guo S (2018) A thermodynamic study of corrosion behaviors for CoCrFeNi-based high-entropy alloys. J Mater Sci 53:14729–14738
40. Chu Z, Shao Z, Guo X, Wu B (2023) Improving corrosion resistance of spark plasma sintering-produced AlCoCrFeNi2. 1 high entropy alloy via in-situ process pressure and temperature control. J Mater Res Technol
41. Ujah C, Popoola A, Popoola O, Aigbodion VS (2020) Influence of CNTs addition on the mechanical, microstructural, and corrosion properties of Al alloy using spark plasma sintering technique. Int J Adv Manuf Technol 106:2961–2969
42. Zhu M, Zhao B, Yuan Y, Guo S, Wei G (2021) Study on corrosion behavior and mechanism of CoCrFeMnNi HEA interfered by AC current in simulated alkaline soil environment. J Electroanal Chem 882:115026
43. Li K et al (2023) Corrosion of eutectic high-entropy alloys: a review. Crystals 13(8):1231
44. Qiu Y, Thomas S, Gibson MA, Fraser HL, Birbilis N (2017) Corrosion of high entropy alloys. npj Mater Degrad 1(1):15
45. Dong P, Vecchiato F, Yang Z, Hooper P, Wenman M (2021) The effect of build direction and heat treatment on atmospheric stress corrosion cracking of laser powder bed fusion 316L austenitic stainless steel. Addit Manuf 40:101902
46. Noell PJ, Sills RB, Benzerga AA, Boyce BL (2023) Void nucleation during ductile rupture of metals: a review. Prog Mater Sci 101085
47. Lister DH, Cook WG (2014) Nuclear plant materials and corrosion, the essential CANDU; Garland, WJ, Ed.; UNENE: Canada
48. Fontana MG, Greene ND (2018) Corrosion engineering. McGraw-hill
49. Ahmad Z (2006) Principles of corrosion engineering and corrosion control. Elsevier
50. Chang S-H, Huang S-P, Wu S-K (2022) Effect of Al content on the selective leaching property of AlxCoCrFeNi high-entropy alloys. Mater Today Commun 32:104079
51. Muangtong P, Rodchanarowan A, Chaysuwan D, Chanlek N, Goodall R (2020) The corrosion behaviour of CoCrFeNi-x (x= Cu, Al, Sn) high entropy alloy systems in chloride solution. Corros Sci 172:108740
52. Licari JJ (2003) Coating materials for electronic applications: polymers, processing, reliability, testing
53. Afseth A, Nordlien J, Scamans G, Nisancioglu K (2002) Effect of thermo-mechanical processing on filiform corrosion of aluminium alloy AA3005. Corros Sci 44(11):2491–2506
54. Campbell J (2016) Consolidation and corrosion of metals: an overview of the role of bifilms in corrosion. Innov Corros Mater Sci (Formerly Recent Patents on Corrosion Science) 6(2):132–139
55. Telegdi J, Shaban A, Trif L (2017) Microbiologically influenced corrosion (MIC). Trends in oil and gas corrosion research and technologies, pp. 191–214
56. Ibrahim A, Hawboldt K, Bottaro C, Khan F (2018) Review and analysis of microbiologically influenced corrosion: the chemical environment in oil and gas facilities. Corros Eng, Sci Technol 53(8):549–563
57. Blackwood DJ (2018) An electrochemist perspective of microbiologically influenced corrosion. Corros Mater Degrad 1(1):59–76
58. Wang J et al. (2023) Effect of Cu content on the microstructure and corrosion resistance of AlCrFeNi3Cux high entropy alloys. Corrosion Science p. 111313
59. Cai Y, Xu Y, Zhao Y, Ma X (2020) Atmospheric corrosion prediction: a review. Corros Rev 38(4):299–321
60. Bardal E (2004) Corrosion and protection. Springer
61. Leygraf C (2002) Atmospheric corrosion, in Corrosion mechanisms in theory and practice: CRC Press, pp. 538–571
62. Cragnolino GA (2021) Corrosion fundamentals and characterization techniques, in Techniques for corrosion monitoring: Elsevier, pp. 7–42
63. Bhandari J, Khan F, Abbassi R, Garaniya V, Ojeda R (2015) Modelling of pitting corrosion in marine and offshore steel structures–a technical review. J Loss Prev Process Ind 37:39–62
64. Li X, Feng Z, Song X, Wang Y, Zhang Y (2022) Effect of hydrogen charging time on hydrogen embrittlement of CoCrFeMnNi high-entropy alloy. Corros Sci 198:110073
65. Nair RB, Arora H, Grewal H (2019) Microwave synthesized complex concentrated alloy coatings: plausible solution to cavitation induced erosion-corrosion. Ultrason Sonochem 50:114–125
66. Dange A (2021) What's new in processing. Available: https://whatsnewinprocessing.co.za/2020/04/15/erosion-corrosion/. Accessed 15 Dec 2023
67. Heppner K, Evitts R, Postlethwaite J (2004) Effect of the crevice gap on the initiation of crevice corrosion in passive metals. Corrosion 60(08)
68. Betts A, Boulton L (1993) Crevice corrosion: review of mechanisms, modelling, and mitigation. Br Corros J 28(4):279–296
69. Melia MA et al (2019) Mechanical and corrosion properties of additively manufactured CoCrFeMnNi high entropy alloy. Addit Manuf 29:100833
70. An X, Chu C, Zhou L, Ji J, Shen B, Chu PK (2020) Controlling the corrosion behavior of CoNiFe medium entropy alloy by grain boundary engineering. Mater Charact 164:110323
71. Li Y, Shi Y (2021) Microhardness, wear resistance, and corrosion resistance of AlxCrFeCoNiCu high-entropy alloy coatings on aluminum by laser cladding. Opt Laser Technol 134:106632

72. Zamanzade M, Barnoush A, Motz C (2016) A review on the properties of iron aluminide intermetallics. Crystals 6(1):10
73. Liu Z, Guo T, Han D, Li A (2020) Experimental study on corrosion-fretting fatigue behavior of bridge cable wires. J Bridg Eng 25(12):04020104
74. Balamurugan A, Rajeswari S, Balossier G, Rebelo A, Ferreira J (2008) Corrosion aspects of metallic implants—an overview. Mater Corros 59(11):855–869
75. Agarwal A, Tyagi A, Ahuja A, Kumar N, De N, Bhutani H (2014) Corrosion aspect of dental implants—an overview and literature review. Open J Stomatol 2014
76. Wang H, Liu P, Chen X, Lu Q, Zhou H (2022) Mechanical properties and corrosion resistance characterization of a novel Co36Fe36Cr18Ni10 high-entropy alloy for bioimplants compared to 316L alloy. J Alloy Compd 906:163947
77. Shang X, Wang Z, He F, Wang J, Li J, Yu J (2018) The intrinsic mechanism of corrosion resistance for FCC high entropy alloys. Sci China Technol Sci 61:189–196
78. Ujah C, Popoola A, Popoola O, Afolabi A, Uyor U (2023) Mechanical and oxidation characteristics of Ti20-Al16-V16-Fe16-Ni16-Cr16 high-entropy alloy developed via spark plasma sintering for high-temperature/strength applications. J Mater Eng Perform 32(1):18–28
79. Wang W-R, Wang W-L, Wang S-C, Tsai Y-C, Lai C-H, Yeh J-W (2012) Effects of Al addition on the microstructure and mechanical property of AlxCoCrFeNi high-entropy alloys. Intermetallics 26:44–51
80. Ujah C, Popoola P, Popoola O, Aigbodion V (2019) Enhanced mechanical, electrical and corrosion characteristics of Al-CNTs-Nb composite processed via spark plasma sintering for conductor core. J Compos Mater 53(26–27):3775–3786
81. He J et al (2014) Effects of Al addition on structural evolution and tensile properties of the FeCoNiCrMn high-entropy alloy system. Acta Mater 62:105–113
82. Firouzdor V, Sridharan K, Cao G, Anderson M, Allen T (2013) Corrosion of a stainless steel and nickel-based alloys in high temperature supercritical carbon dioxide environment. Corros Sci 69:281–291
83. Shi Y, Yang B, Xie X, Brechtl J, Dahmen KA, Liaw PK (2017) Corrosion of Al xCoCrFeNi high-entropy alloys: al-content and potential scan-rate dependent pitting behavior. Corros Sci 119:33–45
84. Kao Y-F, Lee T-D, Chen S-K, Chang Y-S (2010) Electrochemical passive properties of AlxCoCrFeNi (x= 0, 0.25, 0.50, 1.00) alloys in sulfuric acids. Corrosion Sci 52(3):1026–1034
85. Lee C, Chang C, Chen Y, Yeh J, Shih H (2008) Effect of the aluminium content of AlxCrFe1. 5MnNi0. 5 high-entropy alloys on the corrosion behaviour in aqueous environments. Corrosion Sci 50(7):2053–2060
86. Wan X, Lan A, Zhang M, Jin X, Yang H, Qiao J (2023) Corrosion and passive behavior of Al0. 8CrFeNi2. 2 eutectic high entropy alloy in different media. J Alloys Compounds 944:169217
87. Marcus P, Grimal J (1992) The anodic dissolution and passivation of NiCrFe alloys studied by ESCA. Corros Sci 33(5):805–814
88. Newman R, Meng FT, Sieradzki K (1988) Validation of a percolation model for passivation of Fe-Cr alloys: I current efficiency in the incompletely passivated state. Corros Sci 28(5):523–527
89. Chai W, Lu T, Pan Y (2020) Corrosion behaviors of FeCoNiCrx (x= 0, 0.5, 1.0) multi-principal element alloys: role of Cr-induced segregation. Intermetallics 116:106654
90. Tsau C-H, Lin S-X, Fang C-H (2017) Microstructures and corrosion behaviors of FeCoNi and CrFeCoNi equimolar alloys. Mater Chem Phys 186:534–540
91. Kalsar R, Ray RK, Suwas S (2018) Effects of alloying addition on deformation mechanisms, microstructure, texture and mechanical properties in Fe-12Mn-0.5 C austenitic steel. Mater Sci Eng: A729:385–397
92. Shibuya M, Toda Y, Sawada K, Kushima H, Kimura K (2011) Effect of nickel and cobalt addition on the precipitation-strength of 15Cr ferritic steels. Mater Sci Eng, A 528(16–17):5387–5393
93. Fu Y, Li J, Luo H, Du C, Li X (2021) Recent advances on environmental corrosion behavior and mechanism of high-entropy alloys. J Mater Sci Technol 80:217–233
94. Sun X et al. (2021) Mechanical, corrosion and magnetic behavior of a CoFeMn1. 2NiGa0. 8 high entropy alloy. J Mater Sci Technol 73:139–144
95. Qiu X-W, Liu C-G (2013) Microstructure and properties of Al2CrFeCoCuTiNix high-entropy alloys prepared by laser cladding. J Alloy Compd 553:216–220
96. Qiu Y, Thomas S, Fabijanic D, Barlow A, Fraser H, Birbilis N (2019) Microstructural evolution, electrochemical and corrosion properties of AlxCoCrFeNiTiy high entropy alloys. Mater Des 170:107698
97. Wang L et al (2020) Study of the surface oxides and corrosion behaviour of an equiatomic CoCrFeMnNi high entropy alloy by XPS and ToF-SIMS. Corros Sci 167:108507
98. Qiu X, Zhang Y, Liu C (2014) Effect of Ti content on structure and properties of Al2CrFeNiCoCuTix high-entropy alloy coatings. J Alloy Compd 585:282–286
99. Wu C, Zhang S, Zhang C, Zhang H, Dong S (2017) Phase evolution and cavitation erosion-corrosion behavior of FeCoCrAlNiTix high entropy alloy coatings on 304 stainless steel by laser surface alloying. J Alloy Compd 698:761–770
100. Ren B, Zhao R-F, Liu Z-X, Guan S-K, Zhang H-S (2014) Microstructure and properties of Al 0.3 CrFe 1.5 MnNi 0.5 Ti x and Al 0.3 CrFe 1.5 MnNi 0.5 Si x high-entropy alloys. Rare Metals 33:149–154
101. Zhao Y et al (2019) Effects of Ti-to-Al ratios on the phases, microstructures, mechanical properties, and corrosion resistance of Al2-xCoCrFeNiTix high-entropy alloys. J Alloy Compd 805:585–596
102. Öztürk S, Alptekin F, Önal S, Sünbül SE, Şahin Ö, İçin K (2022) Effect of titanium addition on the corrosion behavior of CoCuFeNiMn high entropy alloy. J Alloy Compd 903:163867
103. Zheng H et al (2020) Microstructure evolution, Cu segregation and tensile properties of CoCrFeNiCu high entropy alloy during directional solidification. J Mater Sci Technol 38:19–27
104. Ren B, Liu Z, Li D, Shi L, Cai B, Wang M (2012) Corrosion behavior of CuCrFeNiMn high entropy alloy system in 1 M sulfuric acid solution. Mater Corros 63(9):828–834
105. Nene S et al (2019) Corrosion-resistant high entropy alloy with high strength and ductility. Scripta Mater 166:168–172
106. Wang W et al. (2019) Magnetocaloric effect, corrosion and mechanical properties of Mn1. 05Fe0. 9P0. 5Si0. 5Cux alloys. Intermetallics 113:106539
107. Ujah C, Popoola A, Popoola O, Uyor U (2022) Analysis of the microstructure and tribology of Ti36-Al16-V16-Fe16-Cr16 HEA developed with SPS for engineering applications. JOM 74(11):4239–4249
108. Mondet M, Barraud E, Lemonnier S, Guyon J, Allain N, Grosdidier T (2016) Microstructure and mechanical properties of AZ91 magnesium alloy developed by spark plasma sintering. Acta Mater 119:55–67
109. Soares E et al (2021) Microstructure and mechanical properties of AA7075 aluminum alloy fabricated by spark plasma sintering (SPS). Materials 14(2):430
110. Monchoux J-P, Couret A, Durand L, Voisin T, Trzaska Z, Thomas M (2021) Elaboration of metallic materials by SPS: processing, microstructures, properties, and shaping. Metals 11(2):322
111. Chaim R, Chevallier G, Weibel A, Estournès C (2018) Grain growth during spark plasma and flash sintering of ceramic nanoparticles: a review. J Mater Sci 53:3087–3105

112. Du P, Li B, Chen J, Li K, Xie G (2023) Novel Ti-based bulk metallic glass free of toxic and noble elements for bio-implant applications. J Alloy Compd 934:167996
113. Han Z et al (2020) The corrosion behavior of ultra-fine grained CoNiFeCrMn high-entropy alloys. J Alloy Compd 816:152583
114. Thapliyal S et al (2021) Segregation engineering of grain boundaries of a metastable Fe-Mn-Co-Cr-Si high entropy alloy with laser-powder bed fusion additive manufacturing. Acta Mater 219:117271
115. Parakh A, Vaidya M, Kumar N, Chetty R, Murty B (2021) Effect of crystal structure and grain size on corrosion properties of AlCoCrFeNi high entropy alloy. J Alloy Compd 863:158056
116. Izadi M, Soltanieh M, Alamolhoda S, Aghamiri S, Mehdizade M (2021) Microstructural characterization and corrosion behavior of AlxCoCrFeNi high entropy alloys. Mater Chem Phys 273:124937
117. Ayyagari AV, Gwalani B, Muskeri S, Mukherjee S, Banerjee R (2018) Surface degradation mechanisms in precipitation-hardened high-entropy alloys. NPJ Mater Degrad 2(1):33
118. Thapliyal S et al (2020) Damage-tolerant, corrosion-resistant high entropy alloy with high strength and ductility by laser powder bed fusion additive manufacturing. Addit Manuf 36:101455
119. Research (2024) Perforating gun. Available: https://www.bing.com/images/search?view=detailV2&ccid=4hVfOO3e&id. Accessed 23 Dec 2023
120. Fahrenholtz WG, Wuchina EJ, Lee WE, Zhou Y (2014) Ultra-high temperature ceramics: materials for extreme environment applications. John Wiley & Sons
121. Dabbaghi H, Safaei K, Nematollahi M, Bayati P, Elahinia M (2020) Additively manufactured NiTi and NiTiHf alloys: estimating service life in high-temperature oxidation. Materials 13(9):2104
122. Pullen J, Saeed K (2012) An overview of biodiesel oxidation stability. Renew Sustain Energy Rev 16(8):5924–5950
123. Ujah C, Popoola A, Popoola O, Aigbodion V (2019) Optimisation of spark plasma sintering parameters of Al-CNTs-Nb nano-composite using Taguchi Design of Experiment. Int J Adv Manuf Technol 100:1563–1573
124. Ogunbiyi O, Jamiru T, Sadiku R, Adesina O, lolu Olajide J, Beneke L (2020) Optimization of spark plasma sintering parameters of inconel 738LC alloy using response surface methodology (RSM). Int J Lightweight Mater Manuf 3(2):177–188
125. Olorundaisi E, Babalola BJ, Bayode BL, Teffo L, Olubambi PA (2023) Optimization of process parameters for the development of Ni–Al-Ti-Mn-Co-Fe–Cr high entropy alloy system via spark plasma sintering. Int J Adv Manuf Technol 126(7–8):3323–3337
126. Rameshbabu A, Parameswaran P, Vijayan V, Panneer R (2017) Diffraction, microstructure and thermal stability analysis in a double phase nanocrystalline Al20Mg20Ni20Cr20Ti20 high entropy alloy. J Mech Behav Mater 26(3–4):127–132
127. Raman L et al (2020) Influence of processing route on the alloying behavior, microstructural evolution and thermal stability of CrMoNbTiW refractory high-entropy alloy. J Mater Res 35(12):1556–1571
128. Shen H et al (2019) A novel TiZrHfMoNb high-entropy alloy for solar thermal energy storage. Nanomaterials 9(2):248
129. Sahlberg M, Karlsson D, Zlotea C, Jansson U (2016) Superior hydrogen storage in high entropy alloys. Sci Rep 6(1):36770
130. Chen S-K, Lee P-H, Lee H, Su H-T (2018) Hydrogen storage of C14-CruFevMnwTixVyZrz alloys. Mater Chem Phys 210:336–347
131. Montero J, Zlotea C, Ek G, Crivello J-C, Laversenne L, Sahlberg M (2019) TiVZrNb multi-principal-element alloy: synthesis optimization, structural, and hydrogen sorption properties. Molecules 24(15):2799
132. Karlsson D et al (2018) Structure and hydrogenation properties of a HfNbTiVZr high-entropy alloy. Inorg Chem 57(4):2103–2110
133. G. Popescu et al. (2018) New TiZrNbTaFe high entropy alloy used for medical applications, in IOP Conference Series: Materials Science and Engineering, vol. 400, p. 022049: IOP Publishing
134. Gurel S, Yagci M, Bal B, Canadinc D (2020) Corrosion behavior of novel titanium-based high entropy alloys designed for medical implants. Mater Chem Phys 254:123377
135. Hua N et al (2021) Mechanical, corrosion, and wear properties of biomedical Ti–Zr–Nb–Ta–Mo high entropy alloys. J Alloy Compd 861:157997
136. Sharma N, Alam S, Ray B (2019) Fundamentals of spark plasma sintering (SPS): an ideal processing technique for fabrication of metal matrix nanocomposites, Spark plasma sintering of materials: advances in processing and applications, pp. 21–59
137. Nascimento CB, Donatus U, Rios CT, Antunes RA (2020) Electronic properties of the passive films formed on CoCrFeNi and CoCrFeNiAl high entropy alloys in sodium chloride solution. J Market Res 9(6):13879–13892
138. Zhao Q, Pan Z, Wang X, Luo H, Liu Y, Li X (2022) Corrosion and passive behavior of AlxCrFeNi3− x (x= 0.6, 0.8, 1.0) eutectic high entropy alloys in chloride environment. Corrosion Sci 208:110666
139. Longfei S, Wenbin H, Bokai L, Shan W, Xingpeng G (2023) Corrosion behavior of AlCoCrFeNi2. 1 eutectic high-entropy alloy in Cl--containing solution. J Alloys Compounds 938:168609
140. Kaushik N, Meena A, Mali HS (2022) High entropy alloy synthesis, characterisation, manufacturing & potential applications: a review. Mater Manuf Processes 37(10):1085–1109
141. Wang S-P, Xu J (2017) TiZrNbTaMo high-entropy alloy designed for orthopedic implants: As-cast microstructure and mechanical properties. Mater Sci Eng, C 73:80–89
142. Yang W, Pang S, Liu Y, Wang Q, Liaw PK, Zhang T (2022) Design and properties of novel Ti–Zr–Hf–Nb–Ta high-entropy alloys for biomedical applications. Intermetallics 141:107421
143. Misch CE (2014) Rationale for dental implants. Dental implant prosthetics 2:1–25
144. Wang R et al (2020) Effect of lattice distortion on the diffusion behavior of high-entropy alloys. J Alloy Compd 825:154099
145. Liu C, Wang H, Zhang S, Tang H, Zhang A (2014) Microstructure and oxidation behavior of new refractory high entropy alloys. J Alloy Compd 583:162–169
146. Zhang X et al (2022) The phase composition characteristics of AlCoCrFeNi high entropy alloy heat-treated by simple normalizing treatment and its effects on mechanical properties. J Alloy Compd 926:166896
147. Li J, Fang Q, Liaw PK (2021) Microstructures and properties of high-entropy materials: modeling, simulation, and experiments. Adv Eng Mater 23(1):2001044
148. Zhang Y et al (2014) Microstructures and properties of high-entropy alloys. Prog Mater Sci 61:1–93
149. Sharma DK, Mahant D, Upadhyay G (2020) Manufacturing of metal matrix composites: a state of review. Mater Today: Proc 26:506–519
150. Lee C et al (2020) Lattice-distortion-enhanced yield strength in a refractory high-entropy alloy. Adv Mater 32(49):2004029
151. Pan Q et al (2021) Gradient cell–structured high-entropy alloy with exceptional strength and ductility. Science 374(6570):984–989
152. Li P, Sun H, Wang S, Hao X, Dong H (2020) Rotary friction welding of AlCoCrFeNi2. 1 eutectic high entropy alloy. J Alloys Compounds 814:152322
153. Wu Z, David SA, Feng Z, Bei H (2016) Weldability of a high entropy CrMnFeCoNi alloy. Scripta Mater 124:81–85
154. Newell R, Wang Z, Arias I, Mehta A, Sohn Y, Florczyk S (2018) Direct-contact cytotoxicity evaluation of

CoCrFeNi-based multi-principal element alloys. J Funct Biomater 9(4):59
155. Fischer A, Skreb Y (1980) Cytotoxicity of manganese for mammalian cells in vitro--comparisons with lead, mercury and cadmium. Zentralblatt fur Bakteriologie Mikrobiologie und Hygiene. 1. Abt. Originale B, Hygiene, vol. 171, no. 6, pp. 525–537
156. Lü X, Bao X, Huang Y, Qu Y, Lu H, Lu Z (2009) Mechanisms of cytotoxicity of nickel ions based on gene expression profiles. Biomaterials 30(2):141–148